Review of recent advancements in the lattice QCD determinations of hadron structure

Piotr Korcyl

UNIWERSYTET JAGIELLOŃSKI W KRAKOWIE

Białasówka, AGH, 19 April 2024

NATIONAL SCIENCE CENTRE POLAND This work is supported by NCN grant nr 2022/46/E/ST2/00346.

Outline

Current status based on

- plenary at Lattice2023 by Xiang Gao, Argonne National Laboratory
- plenary at DIS2024 by Huey-Wen Lin, Michigan State University
- recent papers

Plan

- Introduction
- Review of main approaches
- Recent determinations of quark PDF
- Pion and kaon form factors
- Pion distribution amplitude
- Higher-order moments of PDFs
- Evolution

4 **Hadron structure**

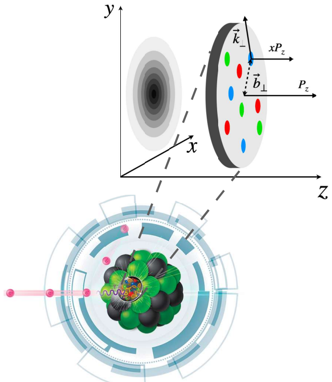

- **The multi-dimensional image of nucleon**

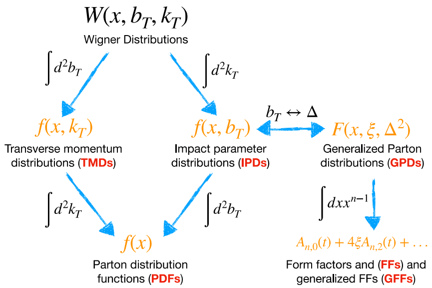

9 **Hadron structure from lattice**

- Moments from Local operator
  - Since the 1980s

$$\bar{q}\gamma^{\{\mu_1}iD^{\mu_2}\dots iD^{\mu_n\}}q$$

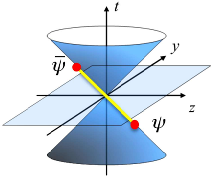

$$\langle p_f|\bar{q}(-\frac{z^-}{2})\gamma^\mu \mathscr{W}(-\frac{z^-}{2},\frac{z^-}{2})q(\frac{z^-}{2})|p_i\rangle$$

Light-cone correlation: Cannot be calculated on the lattice

13 Large momentum effective theory

The quasi distribution from equal-time correlators,

- X. Ji, PRL 110 (2013); SCPMA57 (2014);

$$\tilde{q}(x, P_z, \mu) = \int \frac{dz}{4\pi} e^{-ixP_z z} \langle P | \bar{q}(0) \Gamma \mathscr{W}(0,z) q(z) | P \rangle$$

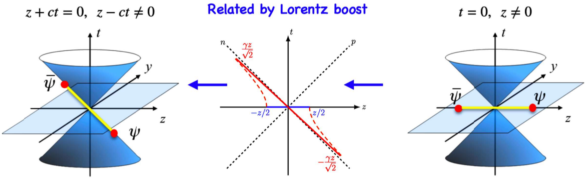

Light-cone: $\langle P | \bar{q}(0) \Gamma \mathscr{W}(0,z^-) q(z^-) | P \rangle$

Quasi: $\langle P | \bar{q}(0) \Gamma \mathscr{W}(0,z) q(z) | P \rangle$

14 Large momentum effective theory

- X. Ji, PRL 110 (2013); SCPMA57 (2014);
- X. Xiong, X. Ji, et al, 90 PRD (2014);
- Y.-Q. Ma, et al, PRD98 (2018), PRL 120 (2018);
- T. Izubuchi, X. Ji, et al PRD98 (2018).
- X. Ji, Y. Zhao, et al, RMP 93 (2021).

Large P_z expansion of quasi distribution:

large P_z is the key

$$\tilde{q}(x, P_z, \mu) = \int \frac{dy}{|y|} C\left(\frac{x}{y}, \frac{\mu}{yP_z}\right) q(y, \mu) + \mathcal{O}\left(\frac{\Lambda^2_{QCD}}{x^2 P_z^2}, \frac{\Lambda^2_{QCD}}{(1-x)^2 P_z^2}\right)$$

- Similar to DIS, DY, ..., LaMET has direct sensitivity to the local $x \in [x_{\min}, x_{\max}]$ dependence instead of the moments.

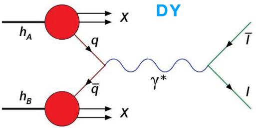

$$\frac{d\sigma}{dQ^2} = \sigma_0 \sum_{a,b} \int \frac{dx_1}{x_1} \int \frac{dx_2}{x_2} q_a^A(x_1, \mu^2)\, q_b^B(x_2, \mu^2)\, \omega_{ab}\left(z, \frac{\mu}{Q}\right)$$

15 **Short distance factorization**

SDF/OPE in z: Ioffe-time pseudo distributions

- V. Braun et al., EPJC 55 (2008)
- A. V. Radyushkin et al., PRD 96 (2017)
- Y. Ma et al., PRL 120 (2018)
- T. Izubuchi et al., PRD 98 (2018)

$$\tilde{h}(z, P_z, \mu) = \tilde{h}(z^2, \lambda, \mu) \qquad \lambda = zP_z$$

$$= \sum_{n=0}^{\infty} \frac{(-izP)^n}{n!} C_n(z^2\mu^2)\langle x^n\rangle(\mu) + \mathcal{O}(z^2\Lambda^2_{\mathrm{QCD}})$$

Sum over the moments

$$= \int_{-1}^{1} d\alpha \, \mathscr{C}(\alpha, \mu^2 z^2) \int_{-1}^{1} dy e^{-iy\lambda} q(y, \mu) + \mathcal{O}(z^2\Lambda^2_{\mathrm{QCD}})$$

- In principle can get access to the higher moments without power divergent mixing.
- In practice the information is limited by the range of finite $\lambda = zP_z$, large P_z essential.

$t = 0, \quad z \neq 0$

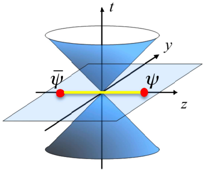

$$\langle P | \bar{q}(0)\Gamma\mathscr{W}(0,z)q(z) | P \rangle$$

$$\mathcal{M}^\alpha(z,P) \equiv \langle P|\bar{\psi}(0)\frac{\lambda_3}{2}\gamma^\alpha \hat{E}(0,z;A)\psi(z)|P\rangle\,, \tag{2.1}$$

where λ_3 is a non-singlet flavor projection and $\hat{E}(0,z;A)$ is the $0 \to z$ straight Wilson line gauge link formed by the gauge field A_μ in the fundamental representation of SU(3). The external hadronic states $|P\rangle$ carry momentum P. A Lorentz covariant decomposition of this matrix element yields:

$$\mathcal{M}^\alpha(z,P) = P^\alpha M(\nu,z^2) + z^\alpha N(\nu,z^2)\,, \tag{2.2}$$

where we have introduced the quantity $\nu = z \cdot P$ known as Ioffe time. In the pseudo-distribution approach, one uses $z = (0,0,0,z_3)$, $\alpha = 0$ and the momentum $P = (P_0,0,0,P_3)$ such that $\mathcal{M}^0(z,P) = P^0 M(\nu,z^2)$, and forms the Lorentz invariant ratio:

$$\mathfrak{M}(\nu,z^2) \equiv \frac{\mathcal{M}^0(z,P)}{\mathcal{M}^0(z,0)}\frac{\mathcal{M}^0(0,0)}{\mathcal{M}^0(0,P)}\,, \tag{2.3}$$

Evolution of parton distribution functions in the short-distance factorization scheme
Hervé Dutrieux, Joseph Karpie, Christopher Monahan, Kostas Orginos and Savvas Zafeiropoulos
11 April 2024

which is finite in the continuum limit, requires no renormalization, and is directly related to the PDF. The fact that the soft physics contained in the z^2-dependent matrix element is similar to that of ordinary PDFs up to higher-twist contributions allows one to interpret these matrix elements as PDFs expressed within another factorization scheme, the SDF. The approach is formalized through a non-local OPE, in which short distance contributions are computed perturbatively, as discussed, e.g., in [4, 8, 10, 15].

As a consequence, the matrix elements computed on the lattice can be related to the Fourier transform of $\overline{MS}$ PDFs by:

$$\mathfrak{M}(\nu, z^2) = \int_0^1 d\alpha\, \mathcal{C}(\alpha, z^2\mu^2, \alpha_s(\mu^2))\, \mathcal{Q}(\alpha\nu, \mu^2) \; + z^2\mathcal{B}(\nu, z^2)\,, \tag{2.4}$$

where $\alpha_s(\mu^2)$ is the strong coupling. $\mathcal{C}(\alpha, z^2\mu^2, \alpha_s(\mu^2))$ is called the matching kernel, computed in perturbation theory, and $\mathcal{Q}(\nu, \mu^2)$ is the (normalized) Ioffe-time distribution (ITD) [27], defined by:

$$\mathcal{Q}(\nu, \mu^2) \equiv \int_{-1}^1 dx\, e^{i\nu x} q(x, \mu^2) \Big/ \int_{-1}^1 dx\, q(x, \mu^2)\,, \tag{2.5}$$

where $q(x, \mu^2)$ is the $\overline{MS}$ PDF. Notice that the ITD is a complex quantity, whose real part probes the x-even part of $q(x, \mu^2)$ and the imaginary part probes the x-odd part of $q(x, \mu^2)$. The term $z^2\mathcal{B}(\nu, z^2)$ in eq. (2.4) captures additional corrections to the leading order

16 x-dependent parton distributions

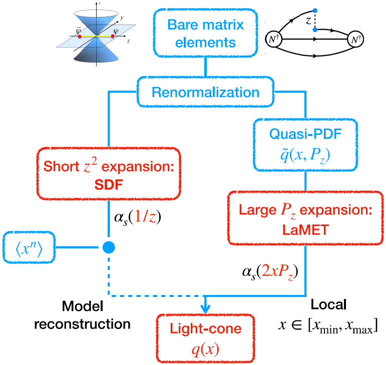

- **What we can compute?**
  - PDFs, GPDs, TMDs ...
- **How well we can compute?**
  - Data precision.
  - Theory/Analysis systematics.

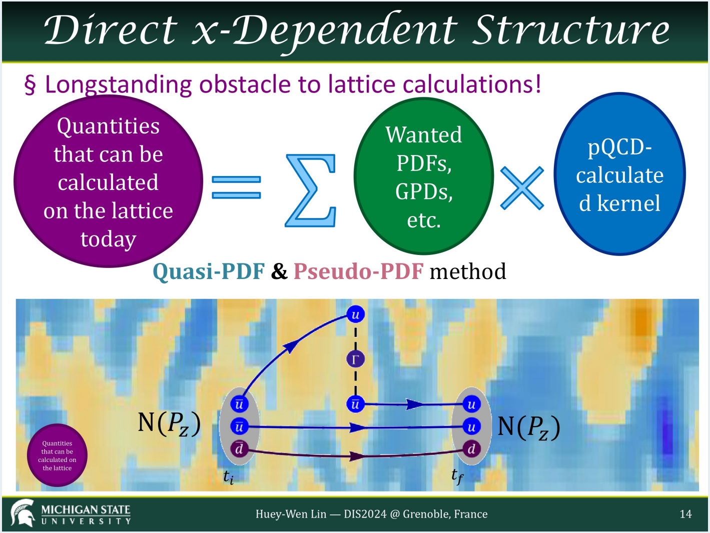
Direct x-Dependent Structure
§ Longstanding obstacle to lattice calculations!
Quantities that can be calculated on the lattice today
=
Σ
Wanted PDFs, GPDs, etc.
×
pQCD-calculated kernel
Quasi-PDF & Pseudo-PDF method
N(P_z)
N(P_z)
u
Γ
$\bar{u}$
$\bar{u}$
$\bar{u}$
$\bar{d}$
u
u
d
t_i
t_f
Quantities that can be calculated on the lattice
MICHIGAN STATE UNIVERSITY
Huey-Wen Lin — DIS2024 @ Grenoble, France
14

30 Towards systematic control

LaMET

Systematics	Continuum	Physical points	$P_z^{\max}$ [GeV]	Renorm.	Matching	DGLAP/ RG	Threshold resummation
Up-to-date calculation	Yes	Yes	2~3 GeV	Hybrid+ LRR	NLO/ NNLO	Yes	In progress

SDF

Systematics	Continuum	Physical points	$P_z^{\max}$ [GeV]	Renorm.	Matching	DGLAP/ RG	Threshold resummation
Up-to-date calculation	Yes	Yes	2~3 GeV	Ratio	NLO/ NNLO	In progress	In progress

- **Data and theoretical precision in good progress.**

Advancements in LQCD determinations of hadron structure

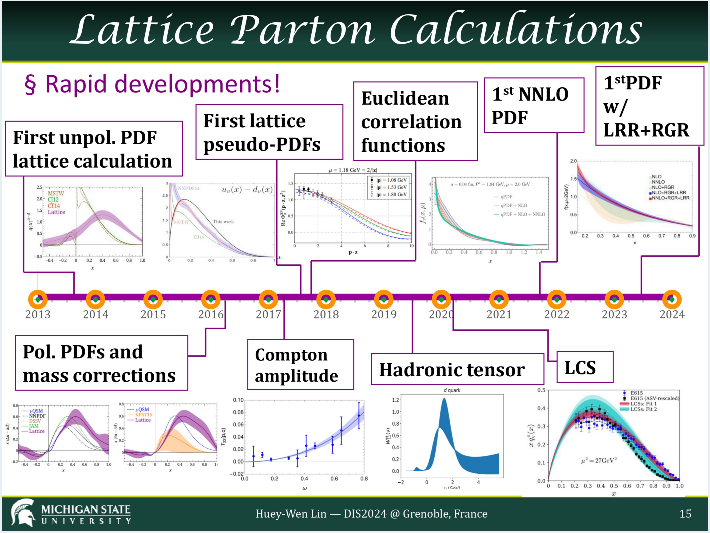

Advancements in LQCD determinations of hadron structure

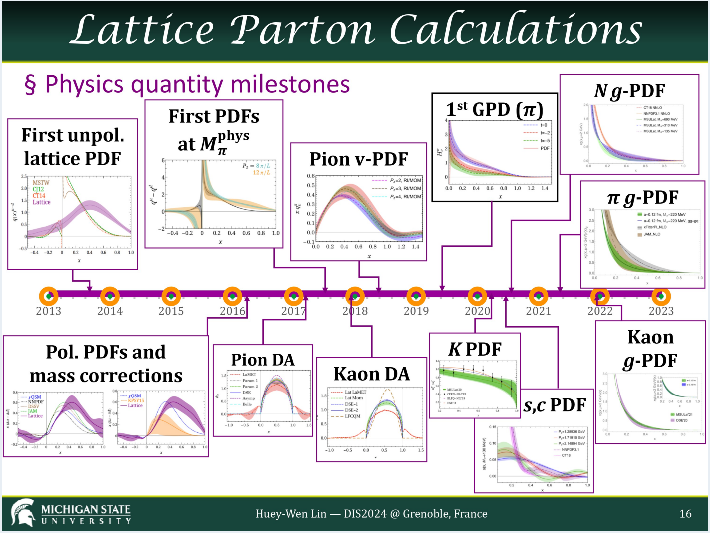

17 Unpolarized quark PDFs

Nucleon unpolarized PDF

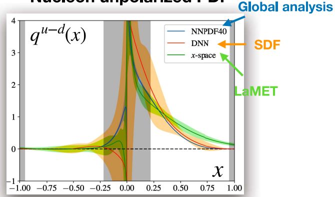

• X. Gao, et al., (BNL+ANL), Phys.Rev.D 107 (2023), 074509

Pion valence quark PDF

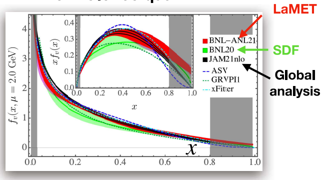

• X. Gao, et al., (BNL+ANL), Phys.Rev.Lett. 128 (2022), 142003

- Unpolarized PDF should be a benchmark.
- Though there are some agreement, lattice results show larger uncertainty and require more precise data and larger momentum.

- Pion has better signal and is easier to approach light-cone with light mass.
- Good agreement with global analysis.

18 Polarized quark PDFs

Helicity

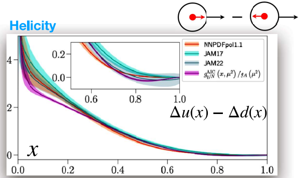

• R. Edwards., (HadStruc Collaboration), JHEP 03 (2023) 086

Transversity

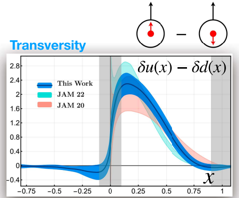

• F. Yao, et al., (LPC), arXiv: 2208.08008

Transversity

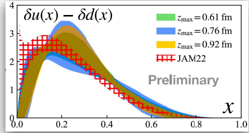

• X. Gao, et al., (BNL+ANL), in preparation.

- Polarized PDFs (helicity, transversity) are also less constrained from experiments.
- Global analysis of transversity (JAM) used the tensor charge from lattice.
- New Lattice calculation could provide more complementary information.

10 Moments from Local operator

Many significant progress such as the form factors (FF), ...

• For review: FLAG Review Eur.Phys.J.C 82 (2022) 10, 869

- **Towards precision calculation of form factor ($Q^2 \lesssim 1\ \mathrm{GeV}^2$), magnetic moments and radius, ...**

Konstantin Ottnad, Mon 2:50 PM

Kohei Sato, Mon 3:10 PM

Miguel Salg, Tue 1:30 PM

Ryutaro Tsuji, Tue 1:50 PM

Aaron Meyer, Tue 2:10 PM

Shigemi Ohta, Tue 2:30 PM

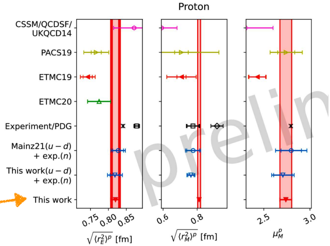

$1.5\ \%$ to $4\ \%$ precision

11 Moments from Local operator

Many significant progress such as the form factors (FF), ...

- Form factors at large momentum transfer $Q^2 \gg 1\ \text{GeV}^2$.

Sergey Syritsyn, Tue 2:50 PM

Qi Shi, Tue 3:10 PM

- Provide the clearest opportunity to study the transition from non-perturbative to perturbative QCD.

- Kaon FF

$m_\pi = 140$ MeV
$m_K = 495$ MeV

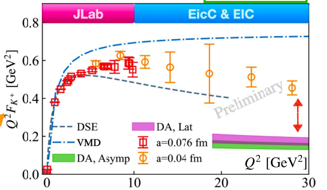

- Q. Shi, X. Gao, et al., (BNL+ANL), in preparation

$$F_\pi(Q^2) \overset{Q^2\to\infty}{=} \mathcal{N}\int_0^1\int_0^1 dxdy\ \phi^*(v,\mu_F^2)$$

$$\times T_F^V(u,v,Q^2,\mu_R^2,\mu_F^2)\phi(u,\mu_F^2) + \mathcal{O}\left(\frac{1}{Q^2}\right)$$

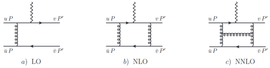

FIG. 1: Sample parton-level Feynman diagrams for the reaction $\gamma^*\pi(P) \to \pi(P')$ at various perturbative orders.

Advancements in LQCD determinations of hadron structure

QCD Predictions for Meson Electromagnetic Form Factors at High Momenta: Testing Factorization in Exclusive Processes
Heng-Tong Ding, Xiang Gao, Andrew D. Hanlon, Swagato Mukherjee, Peter Petreczky, Qi Shi, Sergey Syritsyn, Rui Zhang and Yong Zhao
5 April 2024

In this work, we study the pion and kaon EMFF with large momentum transfers Q2 up to 10 GeV2 and 28 GeV2, respectively, using optimized boosted sources for large momenta in both the initial and final states. Moreover, with independent lattice QCD calculations of the pion and kaon light-cone distribution amplitudes [34–36], as well as the state-of-the-art perturbative input at next-to-next-to-leading order (NNLO) [37], we are able to verify the collinear leading-twist QCD factorization of the EMFF at such high Q2 [6, 7] for the first time, thus demonstrating the universality within these nonperturbative quantities.

25 Large logarithms resummation: LaMET

$$\lim_{\xi\to 1} C\left(\xi,\frac{\mu}{P^z}\right) = 1+\frac{\alpha_s(\mu)C_F}{2\pi}\left[2\frac{\ln|1-\xi|}{|1-\xi|}-\frac{2}{1-\xi}\ln\frac{\mu^2}{(2xP_z)^2}\theta(1-\xi)+\frac{3}{2|1-\xi|}\right] \qquad \xi=\frac{x}{y}$$

- Resum the DGLAP (RG) logs $\ln(\mu^2/(2xP_z)^2)$

$$C(\xi,\frac{\mu}{P_z}) \sim \left(\frac{\alpha_s(2xP_z)}{\alpha_s(\mu)}\right)^{\frac{\gamma_n}{\beta_0}}$$

- The perturbative matching is unreliable at small x $(2xP_z \approx \Lambda_{\rm QCD}$ or $\alpha_s \gtrsim 1)$.
- Enhances the accuracy of the expansion at moderate x $(2xP_z \gtrsim 0.7\ \rm GeV)$.

• Y.S. Su, et al., Nucl.Phys.B 991 (2023) 116201

- Resum large threshold logs $\ln^n|1-\xi|/(1-\xi)$

$$\mathcal{C}\left(\xi,\frac{p^z}{\mu}\right)\Big|_{\xi\to1} = H\left(\frac{4p_z^2}{\mu^2}\right)p^z J_f\left(\frac{(1-\xi)p^z}{\mu},\frac{4p_z^2}{\mu^2}\right)$$

Jet function re-sums the soft gluon exchanges

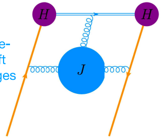

heavy-light Sudakov form factors

- Enhances the accuracy at large x.

• X. Ji, et al., arXiv: 2305.04416.

Threshold resummation for computing large-x parton distribution through large-momentum effective theory
Xiangdong Ji, Yizhuang Liu, Yushan Su
8 May 2023

26 Large logarithms resummation: LaMET

Pion DA

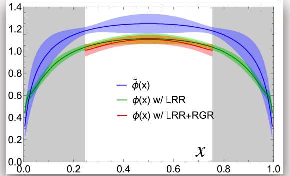

• J. Holligan, et al., Nucl.Phys.B 993 (2023) 116282

- Leading renormalon resummation (LRR) and leading DGLAP (RGR) evolution are included.
- Predict more reliable x dependence in the moderate region with reduced theoretical uncertainty.

Nucleon transversity PDF

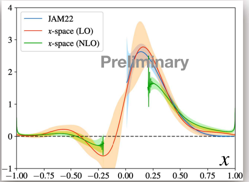

• X. Gao, et al., (BNL+ANL), in preparation.

Toward a precision calculation of GPDs

Jack Holligan, Thu 2:10 PM

The mid-x dependence of the lightcone DA after we perform the inverse matching on the quasi-DA $\phi(x)$. The blue band is the quasi-DA $\tilde{\phi}(x)$ before matching as a reference. We show only $x \in [0.25, 0.75]$ for the result with RGR because the strategy does not work outside the range.

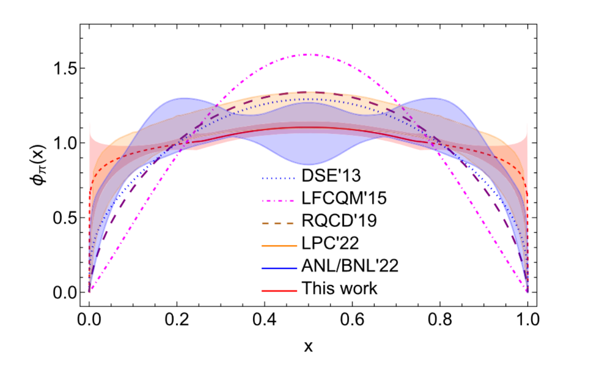

Precision control in lattice calculation of x-dependent pion distribution amplitude
Jack Holligan, Xiangdong Ji, Huey-Wen Lin, Yushan Su, Rui Zhang
1 May 2023

Unlocking higher-order moments of parton distribution functions from lattice QCD

Andrea Shindler

2311.18704 [hep-lat]

shindler@physik.rwth-aachen.de
shindler@lbl.gov

DIS 2024 12.04.2024

Twist-2 operators

$$O_n^{rs}(x) = O_{\mu_1 \cdots \mu_n}^{rs}(x) = \overline{\psi}^r(x)\gamma_{\{\mu_1}\overset{\leftrightarrow}{D}_{\mu_2}\cdots\overset{\leftrightarrow}{D}_{\mu_n\}}\psi^s(x) \qquad \widehat{O}_n^{rs}(x) = Z_n^{\mathrm{MS}}\widehat{O}_{n,\mathrm{B}}^{rs}(x)$$

- Calculate matrix elements using lattice QCD
  - Rotational group symmetry is broken into the hypercubic group H(4)
- Irreducible representations of O(4) generally become reducible representations of H(4) inducing unwanted mixings under renormalization
  - Irreps of H(4) allow mixing with lower dimensional operators and complicate mixings with operators of the same dimension — Beccarini et al.: 1995, Gockeler et al.: 1996
- Operators with different index combinations belong to different irreps of H(4)

O_3

$\mu_1 = \mu_2 = \mu_3$ → $1/a^2\delta_{\mu_i\mu_j}\cos(ap_{\mu_j})$ — Kronfeld, Photiadis: 1985

$\mu_1 \neq \mu_2 = \mu_3$ → $O_{411} - O_{433}$ — Martinelli, Sachrajda: 1987

$\mu_1 \neq \mu_2 \neq \mu_3$ → $\left\langle h(p)|\widehat{O}_n|h(p)\right\rangle = p_{\mu_1}\cdots p_{\mu_n}A_n^h(\mu)$

3

Narayanan, Neuberger:2006

Gradient flow

Lüscher 2010
Lüscher, Weisz 2011

$x_\mu = (\mathbf{x}, x_4) \quad t \to \text{flow-time} \quad [t] = -2$

$A_\mu(x) = A_\mu^a(x) T^a \ \to$ gluon fields

$$\partial_t B_\mu(x,t) = D_\nu G_{\nu\mu}(x,t)$$
$$B_\mu(x,t)|_{t=0} = A_\mu(x)$$

$D_\nu = \partial_\nu + [B_\nu(x,t), \cdot]$

$G_{\mu\nu}(x,t) = \partial_\mu B_\nu(x,t) - \partial_\nu B_\mu(x,t) + [B_\mu, B_\nu]$

$$\partial_t B_\mu = \partial_\nu \partial_\nu B_\mu$$

$$B_\mu(x,t) = \int d^4y\ K(x-y;t) A_\mu(y)$$

$$K(x;t) = \int \frac{d^4p}{(2\pi)^4} \mathrm{e}^{ipx} \mathrm{e}^{-tp^2} = \frac{\mathrm{e}^{-x^2/4t}}{(4\pi t)^2}$$

- Gaussian damping at large momenta
- Smoothing at short distance over a range $\sqrt{8t}$

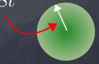

$B_\mu(x,t) \qquad t > 0 \qquad$ finite

Continuum limit is finite

Lüscher, Weisz: 2011

4

Gradient flow

Lüscher: 2013

$x_\mu = (\mathbf{x}, x_4)$ $\quad t \to$ flow-time $\quad [t] = -2$

$$\partial_t \chi(x,t) = \Delta \chi(x,t)$$
$$\partial_t \bar{\chi}(x,t) = \bar{\chi}(x,t) \overleftarrow{\Delta}$$
$$\chi(x, t=0) = \psi(x)$$
$$\bar{\chi}(x, t=0) = \bar{\psi}(x)$$

$\Delta = D_{\mu,t} D_{\mu,t} \qquad D_{\mu,t} = \partial_\mu + B_{t,\mu}$

$$\chi(x,t) = \int d^4y K(x-y,t)\psi(y) \qquad K(x,t) = \frac{1}{4\pi t^2} \mathrm{e}^{-\frac{x^2}{4t}}$$

- Smoothing over a range $\sqrt{8t}$

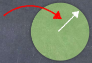

- Gaussian damping at large momenta

$$\chi_R(x,t) = Z_\chi^{1/2} \chi(x,t)$$

$$\mathcal{O}(x,t) = \overline{\chi}(x,t)\Gamma(x,t)\chi(x,t) \qquad \mathcal{O}_R = Z_\chi \mathcal{O}$$

$$\Sigma_t = \langle \overline{\chi}(x,t)\chi(x,t) \rangle \qquad \Sigma_{t,R} = Z_\chi \Sigma_t$$

No additive divergences

Continuum limit finite after normalizing fermion fields

5

Advancements in LQCD determinations of hadron structure

Strategy - Short flow-time expansion

Lüscher: 2013

A.S., Luu, de Vries: 2014-2015
Dragos, Luu, A.S. de Vries: 2018-2019
Rizik, Monahan, A.S.: 2018-2020
A.S.: 2020
Kim, Luu, Rizik, A.S.: 2020
Mereghetti, Monahan, Rizik, A.S., Stoffer: 2021

$$[\mathcal{O}_i(t)]_{\mathrm{R}} = \sum_i c_{ij}(t,\mu)[\mathcal{O}_i(t=0,\mu)]_{\mathrm{R}} + O(t)$$

LQCD   PT - LQCD

$$c_{ij}(t,\mu) = \delta_{ij} + \frac{\alpha_s(\mu)}{4\pi} c_{ij}^{(1)}(t,\mu) + O(\alpha_s^2)$$

- Calculation of matrix elements with flowed fields
  - Multiplicative renormalization (no power divergences and no mixing)
- Calculation of Wilson coefficients
  - Insert OPE in off-shell amputated 1PI Green's functions
- Power divergences subtracted non-perturbatively (LQCD)
- Determination of the physical renormalized matrix element at zero flow-time

6

Strategy

$$\left\langle h(p)|\widehat{\mathring{O}}_n(t)|h(p)\right\rangle = p_{\mu_1}\cdots p_{\mu_n}\left\langle x^{n-1}\right\rangle_h(t)$$

Continuum limit is finite for any n

$$\left\langle x^{n-1}\right\rangle_h^{\mathrm{MS}}(\mu) = c_n(t,\mu)^{-1}\left\langle x^{n-1}\right\rangle_h(t) + O(t)$$

Matching is multiplicative for any n

n=4 $\quad \widehat{O}_{4444} = O_{4444} - \frac{3}{4}O_{\{\alpha\alpha 44\}} + \frac{1}{16}O_{\{\alpha\alpha\beta\beta\}}$

Vanishing spatial momenta for any n

$$\left\langle x^{n-1}\right\rangle_h^{\mathrm{MS}}(\mu) = \left\langle x^{n-2}\right\rangle_h^{\mathrm{MS}}(\mu)\frac{c_{n-1}(t,\mu)}{c_n(t,\mu)}\frac{\left\langle x^{n-1}\right\rangle_h(t)}{\left\langle x^{n-2}\right\rangle_h(t)}, \quad n>2$$

9

Potential systematics

$$\langle x^{n-1}\rangle_h^{\rm MS}(\mu) = \langle x^{n-2}\rangle_h^{\rm MS}(\mu)\frac{c_{n-1}(t,\mu)}{c_n(t,\mu)}\frac{\langle x^{n-1}\rangle_h(t)}{\langle x^{n-2}\rangle_h(t)}, \quad n>2$$

Finite volume effects at finite a the extension of the local operators is (n-1)a $\quad n \sim 10-12$

Discretization errors $\sqrt{8t} \gtrsim na$

- no reason to expect larger cutoff effects than other similar calculations
- ratios are expected to reduce cutoff effects -> effect already observed
- for clover-like fermions ratios contain only O(a²) effects

Perturbative matching $\mu = 2$ GeV

$$c_n^{\rm NLL}(t,\mu,\overline{g}(\mu)) = c_n(t,q,\overline{g}(q))\exp\left\{-\int_{\overline{g}(\mu)}^{\overline{g}(q)} dx\frac{\gamma_n(x)}{\beta(x)}\right\}$$

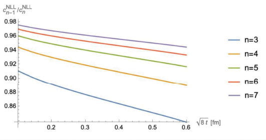

n	$\langle x^{n-1}\rangle$	$\delta_{\rm PT}$
2	$\langle x\rangle$	2%
3	$\langle x^2\rangle$	11%
4	$\langle x^3\rangle$	8%
5	$\langle x^4\rangle$	7%
6	$\langle x^5\rangle$	6%
7	$\langle x^6\rangle$	6%

$\sqrt{8t} = 2(n-1)a$

$a = 0.05$ fm

10

which is finite in the continuum limit, requires no renormalization, and is directly related to the PDF. The fact that the soft physics contained in the z^2-dependent matrix element is similar to that of ordinary PDFs up to higher-twist contributions allows one to interpret these matrix elements as PDFs expressed within another factorization scheme, the SDF. The approach is formalized through a non-local OPE, in which short distance contributions are computed perturbatively, as discussed, e.g., in [4, 8, 10, 15].

As a consequence, the matrix elements computed on the lattice can be related to the Fourier transform of $\overline{MS}$ PDFs by:

$$\mathfrak{M}(\nu,z^2)=\int_0^1 d\alpha\,\mathcal{C}(\alpha,z^2\mu^2,\alpha_s(\mu^2))\mathcal{Q}(\alpha\nu,\mu^2)\;+z^2\mathcal{B}(\nu,z^2)\,, \tag{2.4}$$

where $\alpha_s(\mu^2)$ is the strong coupling. $\mathcal{C}(\alpha,z^2\mu^2,\alpha_s(\mu^2))$ is called the matching kernel, computed in perturbation theory, and $\mathcal{Q}(\nu,\mu^2)$ is the (normalized) Ioffe-time distribution (ITD) [27], defined by:

$$\mathcal{Q}(\nu,\mu^2)\equiv\int_{-1}^1 dx\,e^{i\nu x}q(x,\mu^2)\Big/\int_{-1}^1 dx\,q(x,\mu^2)\,, \tag{2.5}$$

where $q(x,\mu^2)$ is the $\overline{MS}$ PDF. Notice that the ITD is a complex quantity, whose real part probes the x-even part of $q(x,\mu^2)$ and the imaginary part probes the x-odd part of $q(x,\mu^2)$. The term $z^2\mathcal{B}(\nu,z^2)$ in eq. (2.4) captures additional corrections to the leading order

Advancements in LQCD determinations of hadron structure

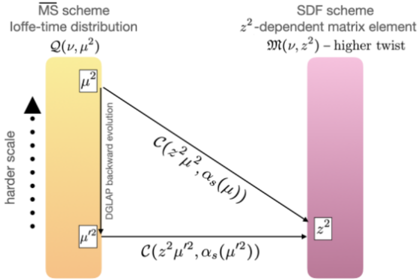

Figure 1. The matching to any scale in $\overline{MS}$ can be performed by dividing the operation into matching to an intermediate scale and evolution to the desired final scale as long as all orders are considered.

Evolution of parton distribution functions in the short-distance factorization scheme
Hervé Dutrieux, Joseph Karpie, Christopher Monahan, Kostas Orginos and Savvas Zafeiropoulos
11 April 2024

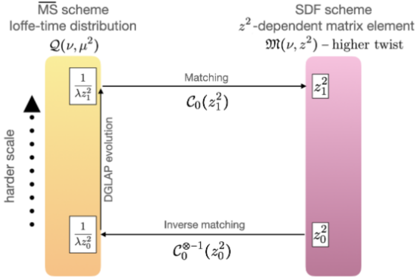

Figure 2. The evolution in SDF depending on z^2 is derived from the $\overline{MS}$ evolution by a back-and-forth matching procedure.

Evolution of parton distribution functions in the short-distance factorization scheme
Hervé Dutrieux, Joseph Karpie, Christopher Monahan, Kostas Orginos and Savvas Zafeiropoulos
11 April 2024

Advancements in LQCD determinations of hadron structure

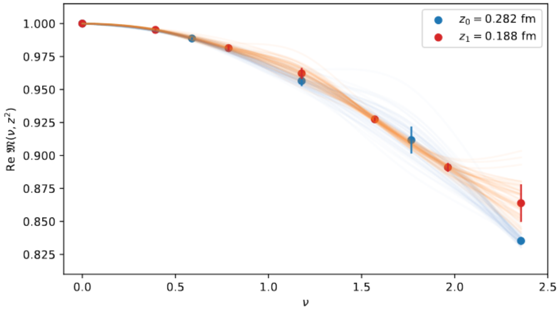

Figure 7. The real part of the isovector proton matrix element $\mathfrak{M}(\nu, z^2)$ published in [52]. The light curves represent 60 cubic splines interpolations of jack-knife samples of the matrix elements.

Evolution of parton distribution functions in the short-distance factorization scheme
Hervé Dutrieux, Joseph Karpie, Christopher Monahan, Kostas Orginos and Savvas Zafeiropoulos
11 April 2024

Our strategy to extract an empirical step-scaling function from the lattice data is first to propose a parametric form of $\Sigma(\alpha; z_0^2, z_1^2)$, and then to fit it to the lattice data:

$$\mathfrak{M}(\nu, z_1^2) = \int_0^1 d\alpha \, \Sigma(\alpha; z_0^2, z_1^2) \mathfrak{M}(\alpha\nu; z_0^2) . \tag{4.1}$$

Evolution of parton distribution functions in the short-distance factorization scheme
Hervé Dutrieux, Joseph Karpie, Christopher Monahan, Kostas Orginos and Savvas Zafeiropoulos
11 April 2024

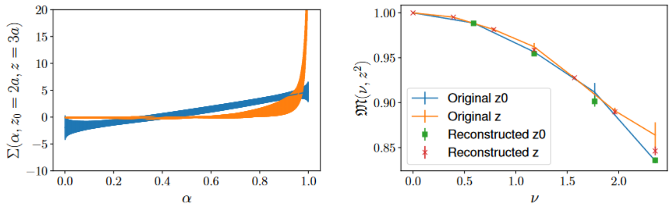

Figure 24. (Left) The step-scaling function from Bayesian Reconstruction (blue) and from the analysis of section 4.3 (orange). The grid consists of 1000 evenly spaced points in α. The prior distribution is defined by $u = 1$ and the smoothness function in eq. (4.4). (Right) The reproduction of the data sets.

Evolution of parton distribution functions in the short-distance factorization scheme
Hervé Dutrieux, Joseph Karpie, Christopher Monahan, Kostas Orginos and Savvas Zafeiropoulos
11 April 2024

That's all

Thank you for your attention!